Journal of Statistical Physics, Vol. 34, Nos. 3/4, 1984

Kinetics of a First-Order Phase Transition: Computer Simulations and Theory

O. Penrose,[1] J. Lebowitz,[2] J. Marro,[3] M. Kalos,[4] and J. Tobochnik[5]

Received August 17, 1983

We make a quantitative comparison between the predictions of the Becker–Döring equations and computer simulations on a model of a quenched binary A-B alloy. The atoms are confined to the vertices of a simple cubic lattice, interact through attractive nearest neighbor interactions, and move by interchanges of nearest neighbor pairs (Kawasaki dynamics). We study in particular the time evolution of the number of clusters of A atoms of each size, at four different concentrations: $\rho_A = 0.035$, 0.05, 0.075, and 0.1 atoms per lattice site. The temperature is 0.59 times the critical temperature. At this temperature the equilibrium concentration of A atoms in the B-rich phase is $\rho_A^{eq} = 0.0145$ atoms/lattice site. The coefficients entering the Becker–Döring equations are obtained by extrapolation from previously published low-density calculations, leaving the time scale as the only adjustable parameter. We find good agreement at the three lower densities. At 10% density the agreement is, as might be expected, less satisfactory but still fairly good—indicating a quite wide range of utility for the Becker–Döring equations.

KEY WORDS: Kinetics; Becker–Doring equations; clusters; computer simulation.

1. INTRODUCTION

The time evolution of macroscopic system from a spatially uniform nonequilibrium state to a nonuniform equilibrium state, consisting of two

Supported in part by NSF Grant DMR81-14726 and DOE Contract DE-AC02-76ERO3077.

[1] Faculty of Mathematics, The Open University, Milton Keynes, England, and Mathematics Department, Rutgers University, New Brunswick, New Jersey.

[2] Department of Mathematics and Physics, Busch Campus, Rutgers University, New Brunswick, New Jersey.

[3] Departamento de Física Teórica, Universidad de Barcelona, Diagonal 647, Barcelona-28, Spain.

[4] Courant Institute of Mathematical Sciences, New York University, New York, New York.

[5] Department of Physics, Worcester Polytechnic Institute, Worcester, Massachusetts 01609.

0022-4715/84/0200-0399$03.50/0

spatially segregated coexisting phases, is a problem of both theoretical and practical interest. Examples of such phenomena are the condensation of liquid droplets from a supersaturated vapor and the segregation by coarsening of binary alloys quenched into the miscibility gap. Our theoretical understanding of these phenomena owes much to the ideas of Becker and Döring. They put forward a system of kinetic equations[1-3] which is intended to describe the time evolution of the size distribution of clusters of minority atoms, assuming the concentration of these atoms to be small.

Past comparisons between the Becker–Döring (BD) theory and observation have been limited to finding the "cloud point," that is, the largest density at which a metastable state is possible. While this involves some extrapolation, the agreement is very satisfactory,[4] and encourages confidence in the theory. This test alone is, however, insufficient to confirm the details of the theory; many features of the kinetics hardly enter into the determination of the cloud point. We therefore felt it worthwhile to test the BD theory more carefully, by comparing its predictions with the results of computer simulations. Such computer "experiments," although they are based on a very simplified version of reality, have some advantages over real experiments. One of these is that, if the density of one of the types of atom is fairly small, the size distribution of clusters of such atoms can be observed as the system evolves. The observed behavior of this distribution can then be compared with the predictions of the BD kinetic equations.

Until recently, quantitative comparisons of this kind were greatly hampered because the equations contain a very large number of unknown coefficients. Recent work[5] has made it possible, however, to calculate values for these coefficients with some degree of confidence. For the coefficients in the equations relating to small clusters (six particles or less) these values were obtained by microscopic calculation, and values for larger clusters can then be obtained by extrapolation. Using these values, therefore, it is now possible to make a detailed comparison between the Becker–Döring equations and the simulations, with a view to identifying the conditions under which these equations, and the assumptions made in calculating the coefficients in them, are valid. It is the purpose of this paper to make such a comparison.

The simulation runs we discuss correspond to a binary alloy on a simple cubic lattice with attractive nearest neighbor interactions. The system is quenched from a very high temperature to a temperature $0.59T_c$, at various overall concentrations of minority atoms: $\rho = 0.035$, 0.05, 0.075, and 0.10. All these concentrations lie between the concentrations of the two phases that can coexist in equilibrium at this temperature; these concentrations are 0.0146 and $1 - 0.0146 = 0.9854$. Therefore each one of our simulation runs is tending towards an eventual equilibrium in which these

two phases coexist in quantities which, for sufficiently large systems, can be calculated from the lever rule. Our interest is in what happens on the way to this final equilibrium.

For reasons which have been discussed elsewhere,[6] the cluster picture underlying the Becker–Döring kinetic equations can be a good description only if the density (concentration) of minority atoms is well below the percolation density, at which a single cluster incorporating a finite fraction of the minority atoms appears soon after the quench or even before it.[7] Even for infinite temperatures, the percolation density is about 30%; and at the lower temperature considered here, which was $0.59T_c$, the density at which a percolating cluster appears immediately after quenching is less than 20%. We therefore did not consider any densities above 10% in the work reported here.

The method by which the runs were obtained is described in Refs. 6 and 8. In Ref. 8 the runs at 5%, 7.5%, and 10% were referred to as P_1, P_2, and P_3. Their durations were 14000, 10200, and 7200 (the time unit being one attempted interchange per site). The run at 3.5%, which was not discussed in Ref. 8, lasted for 16300 attempted interchanges per site.

For the run at 7.5% concentration a comparison with the Becker–Döring equations has already been made in Ref. 5. The method of comparison used here differs from the one used in Ref. 5 in two main respects. One is that here we do not make use of the auxiliary time-dependent parameter l^*, the critical cluster size; this is because there is, in general, no unambiguous method of defining l^*. The other is that here we have not carried out any time averaging of the data before comparing them with the BD predictions; this makes it possible to include in our analysis the rapid changes occurring during the first 300 or so attempted interchanges per site.

2. THE BECKER–DÖRING EQUATIONS

The basic ideas of the BD theory as developed in Refs. 1–3 and 5 are (a) that cluster sizes evolve by the absorption and evaporation of monomers, (b) that the rates of these processes are controlled by the diffusion of monomers, (c) that the monomers near a large cluster are in some sort of local steady state, i.e., the concentration of monomers near a droplet and thus their influx is governed by a finite-difference equation similar to the Laplace equation, and (d) that there is no other spatial correlation between clusters. These assumptions are incorporated into the BD equations, which, in the form we shall use in this paper, are

$$\frac{dc_l}{dt} = J_{l-1} - J_l \qquad (l \geqslant 2) \tag{2.1}$$

where

$$J_l = a_l c_1 c_l - b_{l+1} c_{l+1} \qquad (l \geqslant 1) \tag{2.2}$$

and c_1 is determined from the condition

$$\sum_{l=1}^{\infty} l c_l = \rho = \text{const} \tag{2.3}$$

Here c_l is the concentration of l-particle clusters at time t, ρ is the overal concentration of particles (i.e., of minority atoms), and the kinetic coeffi cients a_l, b_{l+1} are independent of t, though they may depend on the overal density ρ.

The BD theory can be expected to be accurate only in the limiting case of zero density and then only after the system has evolved for a sufficiently long time to establish the local steady state near each of the larger clusters In this limit the kinetic coefficients a_l and b_l can in principle be computed exactly. The method of doing these calculations, and some results for small values of l, are given in Ref. 5. For the temperature $0.59T_c$, the results can be summarized by the approximate formulas

$$a_l \cong D(874 + 1888l)^{1/3} \qquad (\rho \to 0, l \leqslant 6) \tag{2.4}$$

$$b_{l+1}/a_l = w_l \qquad (\rho \to 0) \tag{2.5}$$

where $D = 1/6$ is the zero-density diffusion constant and

$$w_l = Q_l/Q_{l+1} \cong w_s\left[1 + \frac{2.415}{(l-2)^{1/3}}\right] \qquad (3 \leqslant l \leqslant 9) \tag{2.6}$$

with

$$w_s = 0.010526 \tag{2.7}$$

Here Q_l is the cluster partition function defined (for any temperature T) by

$$Q_l = \sum_K e^{-E(K)/kT} \tag{2.8}$$

where the sum goes over all translationally inequivalent l-particle clusters K, $E(K)$ is the energy of cluster K, and k is Boltzmann's constant.

2.1. Extrapolation to Larger l

Before the Becker–Döring equations can be used in practical calculations, these results must be extended to larger values of l and to nonzero densities. For the extension to larger l, direct calculation—though possible in principle—is prohibitively laborious. A natural alternative is to use the formulas in (2.4) and (2.6) for extrapolation, by assuming them to hold for all values of l. Extrapolation is a risky procedure at the best of times, but

we can give it some measure of justification here by two kinds of argument. One is that the behavior of the formulas to leading order in l is what we expect from theory. The other is that there is some agreement between the extrapolation and existing information obtained from computer simulations.

In the case of the formula for w_l, Eq. (2.6), we can check its predictions for large l against those of the standard model used in nucleation theory[2] for temperatures not too close to T_c. That model, treating a cluster of size l as a spherical droplet, gives

$$\log Q_l = -F_l/kT = -(\mu l + \gamma A_l + \cdots)/kT \tag{2.9}$$

where F_l is the free energy of a droplet of size l, μ is the chemical potential on the coexistence line in the phase diagram, γ is the surface tension of the droplet, and A_l is its area. For a spherical droplet the area is

$$A_l = 4\pi R_l^2 = 4\pi\left(\frac{3l}{4\pi\rho_l}\right)^{2/3} \tag{2.10}$$

where R_l is the radius of the droplet and ρ_l is the density within the droplet. If we assume ρ_l to be independent of l, setting $\rho_l = \rho_d = \text{const}$, we obtain from (2.9) and (2.10)

$$\begin{aligned} w_l = Q_l/Q_{l+1} &\cong \exp[\,\mu + \gamma(A_{l+1} - A_l) + \cdots\,]/kT \\ &\cong e^{\mu/kT}\left[1 + \frac{8\pi\gamma}{3kT}\left(\frac{3}{4\pi\rho_d}\right)^{2/3} l^{-1/3} + \cdots\right] \end{aligned} \tag{2.11}$$

The asymptotic form of the extrapolation formula (2.6),

$$w_l = w_s[\,1 + 2.415 l^{-1/3} + \cdots\,] \tag{2.12}$$

thus agrees with this theoretical prediction to the extent that the leading powers of l are the same.

The $l^{-1/3}$ power in (2.12) also agrees with the result of Aizenman, Delyon, and Souillard[16] that $c_l \sim \text{const}\exp(-\text{const}\, l^{2/3})$ for phase coexistence at low temperatures, which indicates [see Eq. (2.14) below] that $Q_l \sim (\text{const})^l \exp(-\text{const}\, l^{2/3})$, and hence, analogously to (2.11), $w_l \sim \text{const}\exp(\text{const}\, l^{-1/3})$.

On the other hand the coefficients in (2.12) do not agree perfectly with (2.9), for example at the temperature $T = 0.59T_c$, which was chosen so as to make $\mu/kT = -4.5$ exactly on the coexistence line in the cubic Ising model, we have $e^{\mu/kT} = e^{-4.5} = 0.01111\ldots$, whereas w_s as given by Eq. (2.7) is about $5\frac{1}{2}\%$ smaller. This particular discrepancy is related to the fact that the saturation density at this temperature, though small (0.0146), is not completely negligible, and the relation between w_s and the fugacity z

$= e^{\mu/kT}$ involves [6] a factor which at low densities is well approximated by $(1-\rho)^4$, i.e., $(1-0.0146)^4$ which is about $5\frac{1}{2}\%$ less than 1. [For further details of this correction, see Section 3 of Ref. 6; but note that the relations between w and z are erroneously given there with a negative exponent for ρ. For example the approximation given there as $w \cong z(1-\rho)^{-4}$ is actually $w \cong z(1-\rho)^4$.]

A quantitative comparison of the coefficient of $l^{-1/3}$ in (2.11) and (2.12) is more difficult since we do not know ρ_d and there are no accurate values for γ. Stauffer *et al.*,[9] working from nucleation rates for metastable states, deduce that the quantity $\Gamma = (36\pi)^{1/3}\gamma/kT\rho_d^{2/3}$ has a value close to 3; this corresponds to a value of 2 for the coefficient of $l^{-1/3}$ in (2.11) agreeing moderately well with the coefficient 2.415 in Eq. (2.12). A more direct approach is to use simulation or series data for γ directly in (2.11). From the results of Leamy *et al.*[10] we estimate that $\gamma/kT \cong 0.5$ so that the coefficient of $l^{-1/3}$ in (2.11) is about $4/3\pi(3/4\pi\rho_d)^{2/3} \cong 1.61\rho_d^{-2/3}$; this agrees with (2.12) if we take $\rho_d \cong 0.5$.

For a more thorough test of the proposed extrapolation formula for w_l we may compare the predictions of this extrapolation with cluster concentrations observed in computer simulations of systems in equilibrium or metastable equilibrium. The most extensive such simulations are those reported by Stauffer *et al.*[9] In the Becker–Döring equations the condition for equilibrium is $J_l = 0$ which, by (2.2) and (2.5), is equivalent to

$$c_1 c_l = w_l c_{l+1} \tag{2.13}$$

The statistical errors in the observed values of c_l for large l are too large to make a direct test of (2.13) useful; instead we replace (2.13) by the equivalent formula

$$c_l = Q_l w^l \tag{2.14}$$

where w is a parameter which in the absence of statistical and finite-density errors would be equal to c_1. Table I shows a test of this equation, using values of c_l taken from the computer simulations of Stauffer *et al.*,[9] the values of Q_l predicted by the extrapolation of w_l using Eq. (2.6), and a value of w obtained from the slope of a graph of $\log(c_l/Q_l)$ against l. The values of c_l correspond to a dimensionless magnetic field $h = 0.44$; this value was chosen because it is large enough to provide measurably large cluster concentrations up to the largest cluster size considered by Stauffer *et al.*, which was 65, yet small enough for this cluster size to be well below the critical cluster size which according to formula (3) of Ref. 9 is about 94 at this reduced magnetic field. The value of w used was $\exp(-4.15) = 0.01576$. Having regard to the random statistical errors affecting the values of c_l, the agreement in the extrapolation range $10 < l \leqslant 65$ does not

Table I. Test of the Extrapolation Formula (2.6) for Q_l/Q_{l+1} by Comparing Observed Values for C_l with Those Predicted by Eq. (2.14)

l	$\ln c_l$	$\ln Q_l$	$\ln Q_l w^l$	Error
1	− 4.25	0	− 4.15	0.1
2	− 5.83	2.599	− 5.70	0.13
3	− 6.89	5.708	− 6.74	0.15
4	− 7.69	9.069	− 7.53	0.16
5	− 8.36	12.553	− 8.20	0.16
6	− 8.95	16.122	− 8.78	0.17
7	− 9.46	19.750	− 9.30	0.16
8	− 9.94	23.424	− 9.78	0.16
9	− 10.38	27.133	− 10.22	0.16
10	− 10.76	30.870	− 10.63	0.13
11	− 11.17	34.632	− 11.02	0.15
12	− 11.49	38.415	− 11.39	0.10
13	− 11.86	42.217	− 11.73	0.13
20	− 13.62	69.221	− 13.78	− 0.16
25	− 15.02	88.806	− 14.94	0.08
30	− 16.12	108.564	− 15.94	0.18
35	− 16.76	128.457	− 16.79	− 0.03
40	− 17.87	148.462	− 17.54	0.33
45	− 18.52	168.560	− 18.19	0.33
50	− 18.61	188.738	− 18.76	− 0.15
55	− 19.21	208.986	− 19.26	− 0.05
60	− 21.01	229.297	− 19.70	1.31
65	− 20.31	249.664	− 20.09	0.22

compare unfavorably with that in the range $1 \leqslant l \leqslant 10$ where Q_l is known exactly.

2.2. Extrapolation of the Formula for a_l to Larger l

Let us now consider the extrapolation of the formula for a_l, Eq. (2.4), to values of l larger than 6. To check the leading power of l we again assume that an l-particle cluster can be modeled as a spherical droplet of radius R_l. The theory of Lifshitz and Slyozov[11,3,5] gives

$$a_l \sim 4\pi D R_l \qquad (\text{large } l) \tag{2.15}$$

where D is the diffusion constant for monomers. In our simulations the low-density value of D is[14] $1/6$, giving

$$a_l \sim \frac{4\pi}{6}\left(\frac{3l}{4\pi\rho_d}\right)^{1/3} = 1.3\rho_d^{-1/3} l^{1/3} \tag{2.16}$$

Eq. (2.4), extrapolated to large values of l, gives

$$a_l \sim 2.06 l^{1/3} \tag{2.17}$$

so that (2.4) and (2.17) can be made to agree for large l by assuming $\rho_d = (1.3/2.06)^3 = 0.25$. This agrees moderately well with the value $\rho_d = 0.35$ estimated from surface tension data earlier in this paper. Another estimate of ρ_d with which to compare these values is the one obtained by Fratzl *et al.*[12] from an analysis of the structure functions in the same simulations. Equation (3.5) of their paper corresponds to the estimate $\rho_d \cong 0.5$. There are, it is true, grounds for doubting the assumption of spherical clusters,[3] but at present not enough is known about the shapes of large clusters to lead to a useful formula to replace the simple $l^{1/3}$ law predicted by (2.4) or (2.17).

Some further support to the $l^{1/3}$ hypothesis is given by the analysis carried out previously by us[14] on the time-dependent distribution of large clusters observed in the simulation run at 7.5% density. In that analysis a quantity A was defined by

$$A = 2.415 w_s (1-\rho)^3 \alpha \tag{2.18}$$

where ρ is the density, $2.415 w_s$ is the coefficient of $l^{-1/3}$ in (2.6), and α is defined by $a_l \sim \alpha l^{1/3}$; it was found that the simulation data for times between about 1000 and 6000 attempted interchanges per site indicated a value $A = 0.15$, which corresponds to $\alpha = 7.5$, i.e.,

$$a_l \sim 7.5 l^{1/3} \tag{2.19}$$

The fact that the analysis worked at all is some confirmation for the $l^{1/3}$ law; the fact that this "observed" coefficient of $l^{1/3}$ is 3 or 4 times as big as the extrapolated value has already received some discussion in Ref. 5 and we shall return to it.

2.3. Corrections for Nonzero Density

It remains to discuss the modifications of our extrapolation formulas (2.4) and (2.6) made necessary by the fact that the density is not zero. In the case of the formula for w_l, we shall follow the convention used in Ref. 5 which is to leave w_l unaltered but to multiply it in the right-hand side of (2.5) by a power of $1-\rho$; the replacement used there, derived from the empirical formula for equilibrium cluster numbers given in Ref. 6, is

$$\frac{b_{l+1}}{a_l} = \begin{cases} (1-\rho)^2 w_l & (l=1) \\ (1-\rho)^3 w_l & (l \geqslant 2) \end{cases} \tag{2.20}$$

An alternative replacement, based on the more accurate empirical formula

for the equilibrium cluster numbers given by Marro and Toral[15] would be

$$\frac{b_{l+1}}{a_l} = \begin{cases} (1-\rho)^2 w_l & (l=1) \\ (1-\rho)^{2.75} w_l & (l=2) \\ (1-\rho)^{3.25} w_l & (l \geqslant 3) \end{cases} \tag{2.21}$$

However, we found that replacing (2.20) by (2.21) affected the solution to the BD equations by an amount which was small in comparison with the differences between these solutions and the simulation data; consequently, we used the simpler formula (2.20) for our main series of BD runs which is reported in this paper.

The extrapolation of Eq. (2.20) to large values of l can be tested against simulation data in the same way as that of Eq. (2.5): by comparing it with the simulation data of Stauffer *et al.*[9] recorded in Table I. The analog of Eq. (2.14) is now

$$c_l = (1-\rho)^4 Q_l w^l \qquad (l \geqslant 2) \tag{2.22}$$

where w is a parameter which in the absence of statistical errors would be equal to $c_1(1-\rho)^{-3}$. This formula can be tested using the data in Table I. The appropriate value of ρ, deduced from the cluster concentrations observed in the simulation, is 0.029, and so the values of $\ln[(1-\rho)^4 Q_l w^l]$ can be obtained by adding $\ln(1-0.029)^4 = -0.12$ to the values of $\ln Q_l w^l$ given in the table. Values for the error $\ln[(1-\rho)^4 Q_l w^l] - \ln c_l$ can be obtained by adding -0.12 to the numbers in the column marked "error." For $l \leqslant 13$ these error values are clearly smaller than the ones shown in the table which apply to the $\rho = 0$ formula (2.14). For larger values of l the comparison is more difficult, since neither formula fits the data very accurately, but the change from (2.14) to (2.22) reduces the magnitudes of more errors than it increases. Probably these errors are mainly statistical errors in the data, and so the extrapolation of Eq. (2.20) to large values of l does not appear to be inconsistent with the information given by the simulation.

Finally we consider what change should be made in Eq. (2.4), the formula for a_l, when the density is finite. At finite densities the transport of matter in the neighborhood of a given large cluster is due not only to the diffusion of monomers but also to processes involving dimers, trimers, etc. Therefore we may expect this transport to be faster than in the zero-density limit, when the numer of dimers, trimers, etc. is negligible. In the absence of any quantitative theory of such effects we took them into account by the expedient of allowing the factor D in Eq. (2.4) to depend on the density in a purely empirical way; that is, we treated D as an adjustable parameter whose value was chosen separately at each density considered so as to give

the best agreement between the BD equation and the simulation data. This procedure, while not totally successful in the case of the runs at density 10%, is simple to apply to data plotted on a logarithmic time scale, and is much more consistent with the data than the alternative suggestion made in Ref. 5 of allowing D to depend on c_1 rather than on the overall density.

3. THE CALCULATIONS

For our numerical calculations we used the Becker–Döring equations (2.1)–(2.3), with a_l given by (2.4) and b_l by (2.6) with (2.20). They were first reduced to a finite system by choosing a suitable integer L, setting $J_L = 0$, and treating (2.1) as a system of equations for the $L - 1$ variables $c_2 \ldots c_L$ [since c_1 can be expressed in terms of $c_2 \ldots c_L$ using (2.3)]. It is not necessary for L to be constant: it can increase with t, and when it increases the new variables c_l created thereby can initially be set equal to zero. The equations were solved using the trapezoidal method, the nonlinear system of $L - 1$ algebraic equations arising at each step being solved iteratively by the Newton–Raphson method, using the values from the previous step as first approximation. Provided L was chosen large enough at each time step to make c_L negligibly small, only one Newton–Raphson iteration was usually necessary. For small values of t step sizes as small as 0.01 were used, but then L could be chosen quite small, e.g., 20 or 50, so that the amount of time required to advance the calculation to the next required t value was less than a minute. For larger values of t (1000 or more) it was generally necessary to user larger values of L (up to 3000), but by this time step sizes as large as 100 or even more were practicable without instability or serious loss of accuracy, so that the calculations still went fairly quickly. They were carried out on the VAX-11/780 computer at Rutgers University.

4. COMPARISON OF THEORY AND SIMULATION

4.1. Density 3.5%

Table II shows data from our simulation run at density 3.5%, the earlier part of which has already been described qualitatively by Kalos *et al.*[6] In our tables and figures, the symbol c_l means the number of clusters on the $50 \times 50 \times 50$ lattice used for our simulations; this is 125000 times as large as the quantity denoted by c_l in Section 2 of the paper. The notation c_l^m means the number of clusters of sizes l through m, i.e., $c_l + c_{l+1} + \cdots + c_m$; and N_l^m means the number of particles in clusters of sizes

Table II. Simulation Data at 3.5% Density

t	c_1	c_2	c_3	c_4	c_5	c_6	c_7	c_8	c_9	c_{10}	c_1^{10}	c_{11}^{20}	c_{21}^{50}	c_{51}^{100}	N_1^{10}	N_{11}^{20}	N_{21}^{50}	N_{51}^{100}
0	3447	362	57	7	1						3874				4375			
1.4	2702	519	143	31	10	3	2				3410				4375			
2.8	2500	544	165	38	19	4	3				3273				4375			
4.4	2322	558	169	63	21	8	1	1	0	1	3144				4375			
6.0	2249	533	164	76	35	6	5	0	2	0	3070	0			4375			
9.1	2193	494	182	88	29	15	2	2	1	0	3006	2			4353	22		
12.5	2087	485	189	77	40	26	7	2	0	1	2914	1			4363	12		
15.8	2045	479	178	76	38	20	21	6	2	0	2865	1			4364	11		
19.2	2076	457	153	80	52	22	18	6	2	1	2867	1			4363	12		
29.2	2064	469	170	69	43	19	15	8	3	4	2864	2			4353	22		
50.2	1906	455	178	80	37	27	16	11	7	2	2719	6			4300	75		
763	1919	421	153	70	48	26	19	12	10	3	2681	10			4245	130		
103	1856	429	169	74	55	22	13	14	6	3	2641	12			4211	164		
148	1921	409	163	92	36	28	19	16	4	6	2694	4	1		4301	53	21	
195	1926	414	168	72	42	25	16	10	4	5	2682	14	0		4184	191		
295	1825	432	170	80	37	33	17	7	12	6	2619	10	0		4245	130		
494	1867	415	162	65	45	20	10	8	6	6	2604	22	2		4036	286	53	
710	1870	405	140	75	50	26	11	11	4	6	2598	14	4		4067	190	118	
999	1890	402	159	56	39	30	11	9	10	6	2612	16	3		4069	221	85	
1505	1909	387	155	76	41	20	10	9	9	4	2620	18	3		4040	249	86	
1992	1913	467	140	65	40	21	9	10	2	6	2673	17	2		4074	227	74	
3027	1838	419	151	75	39	26	13	8	3	3	2575	19	2	1	3992	273	59	51
4976	1819	395	158	77	51	22	16	9	6	5	2558	14	5	0	4066	178	131	
7497	1931	402	148	79	35	32	23	6	5	4	2665	12	2	0	4156	169	50	
10030	1846	384	159	77	50	25	13	9	8	5	2576	10	1	2	4084	134	41	116
16288	1823	414	150	87	55	24	16	9	5	5	2588	12	5	0	4147	104	124	

l through m, i.e., $lc_l + (l+1)c_{l+1} + \cdots + mc_m$. Started at time 0 from a distribution corresponding to infinite temperature, the system settles down after about 1000 time steps into a state where few large clusters are present and no systematic change with time is discernible, even though the simulation was continued out to time 16300. That is, we have a one-phase state, apparently stationary; yet the density 3.5% is well above the maximum density (1.46%) that is possible for a single low-density phase in equilibrium at this temperature. We therefore interpret the state attained by the system after time 1000 as a metastable state.

A comparison of these data with the prediction of the Becker–Döring equations is shown in Fig. 1. The time axis used for plotting the Becker–Döring equations has been shifted by a factor of 2.5; this is equivalent to saying that the factor D used in Eq. (2.4) is given the value $5/12$ in place of $1/6$. With this modification, and having regard to the large fluctuations in the value of c_{11}^{20}, the BD equations agree well with the simulation results over a wide time range from about 5 attempted interchanges per site to about 10000. The largest systematic discrepancy is the behavior of c_2 for times less than 10: the BD equations overestimate some of the values of c_2 in this time range by 10% to 20%.

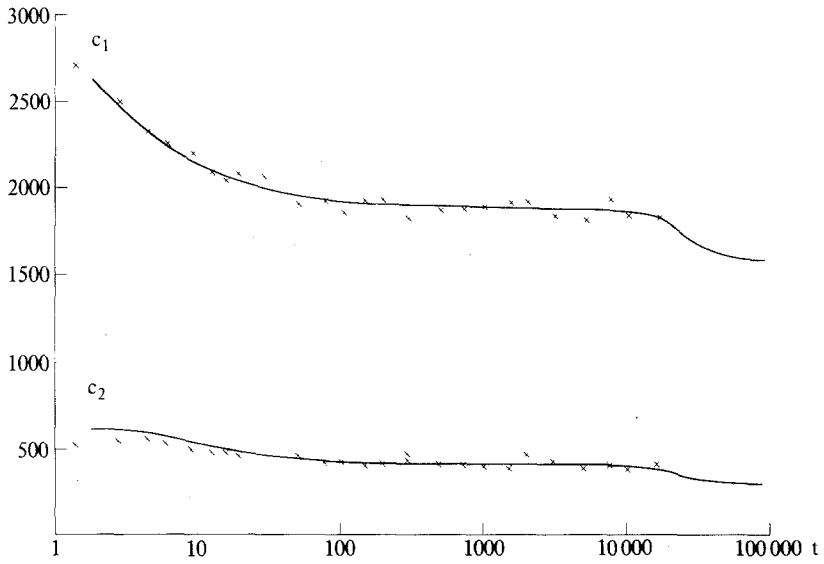

(a)

Fig. 1. Comparison of simulation data (crosses) with predictions of the Becker–Döring equations (curves) at 3.5% density.

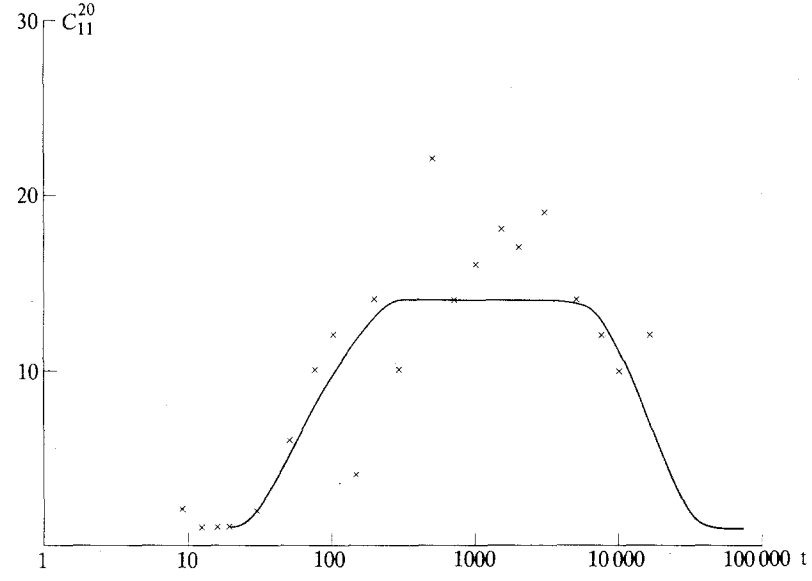
30
C_{11}^{20}
20
10
1
10
100
1000
10 000
100 000 t

(b)

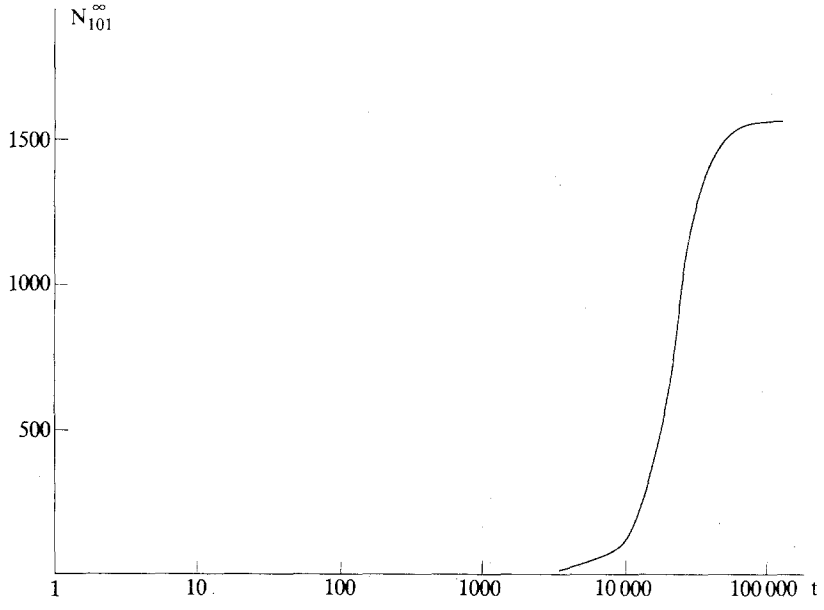
N_{101}^{∞}
1500
1000
500
1
10
100
1000
10 000
100 000 t

(c)

Table III. Simulation Data at Density 5%

t	c_1	c_2	c_3	c_4	c_5	c_6	c_7	c_8	c_9	c_{10}
0	4589	584	115	24	4	3	2	0	0	0
5.6	2580	703	311	131	66	28	21	7	4	3
12.0	2264	594	284	161	82	54	21	20	11	3
18.7	2203	590	261	144	81	66	29	13	13	8
25.4	2220	566	249	130	85	39	39	19	17	10
39.2	2133	529	235	126	67	49	36	28	17	12
53.2	2090	502	213	134	72	53	35	21	16	23
81.6	2059	507	217	91	71	45	25	29	22	16
96.0	2085	482	201	99	75	41	30	21	19	15
155	1925	464	197	107	73	42	23	22	17	14
200	1931	463	209	91	64	35	36	16	18	17
304	1987	430	202	84	65	36	27	19	15	9
500	1884	448	177	103	62	31	21	15	9	5
743	1980	428	173	82	58	39	21	18	15	6
1003	1992	464	170	102	58	22	21	18	8	12
1506	1894	463	160	70	34	37	17	19	11	11
2004	1909	433	162	70	35	25	18	13	10	12
3008	1858	393	152	75	39	26	17	16	11	6
4997	1794	368	109	50	38	16	14	11	4	3
7496	1657	306	88	47	32	12	2	3	2	1
10000	1585	276	86	42	13	14	2	2	3	2
13976	1551	297	83	40	10	8	4	1	2	0

Although the Becker–Döring equations reproduce the observed cluster size distributions quite well for $t < 10{,}000$, it is not so clear whether they would do so for larger times. The equations show a slow but steady decrease in c_1, the number of monomers, during the time interval from about 100 to 10,000 at a rate of roughly 1 monomer per 300 time steps. Since there are only about 2000 monomers present, this decrease indicates that the lifetime of the metastable state cannot be more than $2000 \times 300 = 600{,}000$ time steps, and in fact the equations show c_1 changing more rapidly after about 10,000 time steps so that the metastable state may be said to cease at about this time. This behavior is clearly shown by the third graph in Fig. 1, according to which N_{101}^{∞}, the number of particles in clusters sized at least 101, which should be very small for a metastable state, grows rapidly after time 10,000. The simulations neither confirm nor contradict this picture. One would expect an eventual break-up of the metastable state, but there is no evidence foreshadowing it in the simulation data up to time 16288, so that the lifetime of the metastable state in this particular run may be considerably greater than that indicated by the BD equations. Possibly the finite size of the system used in the simulation run makes

Table III. (Continued)

t	c_1^{10}	c_{11}^{20}	c_{21}^{50}	c_{51}^{100}	c_{101}^{500}	c_{501}^{00}	N_1^{10}	N_{11}^{20}	N_{21}^{50}	N_{51}^{100}	N_{101}^{500}	N_{501}^{00}
0	5321	0	0	0	0		6250	0				
5.6	3854	3					6210	40				
12.0	3494	10					6118	132				
18.7	3408	17					6047	203				
25.4	3374	21	1				5956	272	22			
39.2	3232	36	0				5778	472	0			
53.2	3159	35	3				5734	450	66			
81.6	3082	51	3				5478	688	84			
96.0	3068	60	3				5368	805	77			
155	2884	60	10				5119	863	268			
200	2880	52	16				5090	740	420			
304	2874	48	25				4896	705	649			
500	2755	52	28	2			4617	696	818	119		
743	2820	40	25	4			4693	577	754	226		
1003	2867	37	15	7			4743	528	488	491		
1506	2716	31	15	12			4452	429	479	890		
2004	2687	23	20	7	5		4306	330	552	487	575	
3008	2593	22	10	3	8		4157	318	310	209	1256	
4997	2407	8	2	2	10		3595	114	81	153	2307	
7496	2150	2	1	2	8	1	3019	25	22	190	2476	518
10000	2025	1	2	0	7	2	2789	11	45	0	2145	1260
13976	1996	1	0	0	5	4	2706	14	0	0	959	2571

break-up of the metastable state less likely than it would be in the infinite system modelled by the BD equations.

4.2. Density 5%

Data from the 5% simulation run are shown in Table III. The early part of this run was described qualitatively by Kalos *et al.*[6] The main new phenomenon is the formation of a sizable population of "large" clusters (i.e., clusters containing more than about 10 particles) during times between about 10 and 500; this population then decreases again, but the sizes of the clusters remaining in it grow so that the total number of particles in large clusters continues to grow.

Figure 2 shows a graphical comparison of the simulation data with Becker–Döring calculations for 5% density, using a time rescaling factor of 3, which corresponds to taking $D = \frac{1}{2}$ in Eq. (2.4). The agreement for concentrations of small clusters is about as good as for 3.5%, but the BD equations are now called upon to make predictions about the large clusters as well. Here the agreement is somewhat worse; the number of large

Table IIIa. Additional Simulation Data at 5% Density

t	c_1	c_2	c_3	c_4	c_5	c_6	c_7	c_8	c_9	c_{10}	c_1^{10}	c_{11}^{20}	c_{21}^{50}
0	4509	594	123	31	10	2	0				5268		
0.5	3710	766	207	58	21	3	3				4760		
1	3358	785	243	89	28	8	4	1			4524		
1.5	3098	772	278	109	33	17	6	2			4315		
2	2968	768	285	111	42	15	14	2	2		4207	1	
3	2737	759	285	120	59	27	15	6	3	1	4012	1	
5	2554	713	299	124	74	37	13	15	0	2	3031	4	
7.5	2445	661	306	136	63	47	21	12	8	4	3703	5	
10	2394	604	250	171	79	34	26	17	5	8	3588	14	
15	2208	548	280	147	79	49	32	18	11	6	3378	23	
20	2148	563	274	135	84	49	38	19	8	7	3325	25	0
25	2156	583	221	133	86	49	42	21	15	7	3313	23	2
50	2017	540	226	127	74	48	43	28	15	15	3133	36	2
75	2039	507	213	128	85	49	29	26	23	19	3118	30	5
100	2008	505	193	103	87	51	32	20	11	12	3022	52	7
150	1991	485	208	98	65	46	36	25	17	12	2983	47	12
200	1935	468	203	105	74	42	34	17	21	14	2913	47	13
300	2009	485	198	89	71	41	28	26	10	9	2966	61	11

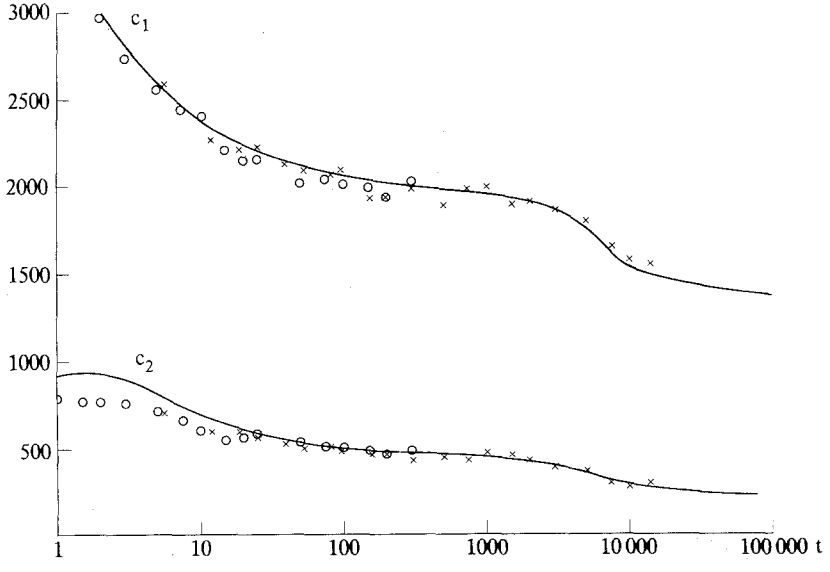

(a)

Fig. 2. Comparison of data from two independent simulation runs (crosses and circles) with predictions of the Becker–Döring equations (curves) at 5% density. The dotted lines are to guide the eye only.

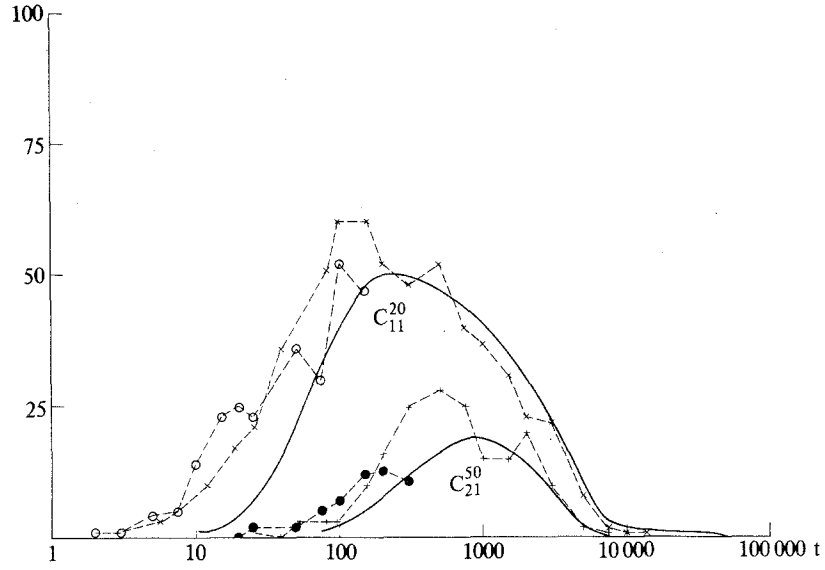
100
75
50
25
C_{11}^{20}
C_{21}^{50}
1
10
100
1000
10 000
100 000 t

(b)

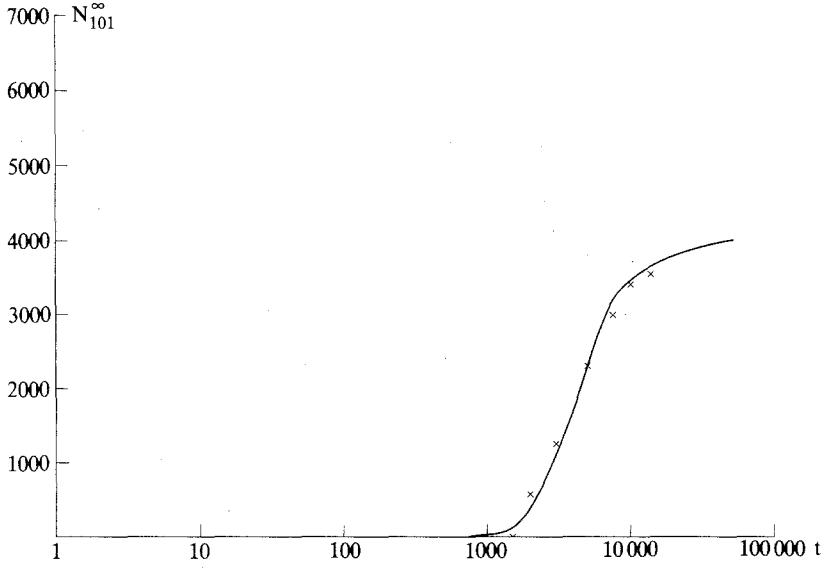
7000
N_{101}^{∞}
6000
5000
4000
3000
2000
1000
1
10
100
1000
10 000
100 000 t

(c)

Table IV. Simulation Data at Density 7.5%

t	c_1	c_2	c_3	c_4	c_5	c_6	c_7	c_8	c_9	c_{10}
0	5790	965	310	88	35	11	11	4	1	0
4.1	2732	936	416	252	148	101	48	34	17	10
8.9	2474	715	374	189	157	109	58	48	32	34
14.0	2219	657	334	185	129	94	75	68	40	29
19.4	2121	655	290	180	126	105	69	65	45	31
30.1	2128	582	293	149	126	81	74	60	36	39
52.4	2043	568	243	137	108	82	60	37	47	30
75.6	1984	484	223	162	85	57	40	50	32	28
99.3	1971	511	197	133	79	60	49	36	25	31
147	1961	499	218	128	83	51	39	27	28	18
197	1963	489	195	104	73	42	28	34	18	20
298	1850	445	173	113	52	49	25	20	22	12
494	1786	428	171	87	46	47	26	20	21	15
753	1877	388	141	83	56	30	15	17	11	13
1006	1838	358	156	79	60	24	28	9	14	13
1501	1691	357	128	72	35	18	15	15	14	4
1997	1612	381	113	70	46	21	7	7	7	4
3002	1639	304	119	64	22	18	7	5	3	4
5004	1514	263	76	48	16	6	6	4	0	1
7504	1494	296	89	29	17	7	4	1	0	1
10199	1461	283	86	35	17	13	5	0	2	0

clusters grows about twice as fast as predicted by the BD equations with the time scaling we have used (in the sense that any given value is reached twice as early as the equations predict) and the maximum number of clusters containing more than 20 particles is about 50% greater than predicted. On the other hand the BD equations are fairly successful in predicting the distribution of large clusters after the time at which this maximum is reached.

As in the case of 3.5% density, the BD equations show the number of monomers decreasing steadily between times 100 and 10,000; but this time the rate of decrease is much faster, about 1 monomer per 50 time steps, and there is at best a rather fleeting period of approximate constancy in c_1 which does not last beyond about $t = 2000$. After this time the decreasing character of c_1 is strong enough to be quite clear even in the simulation data, and there is agreement between the simulation and the BD equations about the time at which this "metastable" behavior comes to an end.

The last graph in Fig. 2 shows that the BD equations give a good representation of the observed time variation of N_{101}^{∞}, thereby increasing one's confidence that the late increase in N_{101}^{∞} predicted by the BD

Table IV. (Continued)

t	c_1^{10}	c_{11}^{20}	c_{21}^{50}	c_{51}^{100}	c_{101}^{500}	c_{501}^{5000}	N_1^{10}	N_{11}^{20}	N_{21}^{50}	N_{51}^{100}	N_{202}^{500}	N_{501}^{5000}
0	7215	1					9361	14				
4.1	4694	22	1				9067	286	22			
8.9	4190	55	1				8639	713	23			
14.0	3830	77	6				8203	1030	142			
19.4	3687	98	3				7999	1293	83			
30.1	3568	109	12				7595	1491	289			
52.4	3355	125	27				6927	1735	713			
75.6	3145	129	45				6284	1875	1216			
99.3	3092	134	51	1			6037	1909	1375	54		
147	3052	99	59	7			5767	1476	1696	436		
197	2966	91	66	11			5389	1295	1998	693		
298	2761	89	63	16	1		4918	1320	1958	1064	115	
494	2647	61	57	28	1		4696	890	1814	1872	103	
753	2631	46	43	27	9		4338	683	1395	1807	1152	
1006	2579	27	29	27	13		4306	378	940	1908	1843	
1501	2349	21	18	14	24		3751	294	665	953	3712	
1997	2268	17	11	8	25		3557	248	381	551	4638	
3002	2185	7	6	6	22		3234	83	227	513	5318	
5004	1934	1	1	3	21	1	2660	12	47	220	5750	686
7504	1938	0	1	0	19	1	2642	0	25	0	5976	731
10199	1902	1	1	1	14	4	2641	11	38	74	4246	2364

equations for 3.5% density would also be observed in the simulations if they were continued longer.

4.3. Density 7.5%

Data from the 7.5% simulation run are shown in Table IV. This run has already been subjected to extensive analysis by Penrose *et al.*[13] and by Penrose and Buhagiar.[5] The main difference from the 5% case is that the population of large clusters is much bigger and builds up more quickly.

Figure 3 shows a graphical comparison of the simulation and the predictions for 7.5% density. In plotting Fig. 3 we used a scaling factor of 6, which is equivalent to giving the factor D in our formula (2.4) for a_l the value 1 instead of 1/6. With this adjustment, the agreement between theory and simulation is at least as good as at density 5%: the predicted growth of the number of large clusters in any particular size range is still too slow by a factor of roughly 2, but the maximum values reached are predicted fairly well. At this density it makes no sense to talk of even a short-lived metastable state; instead c_1 decreases steadily from start.

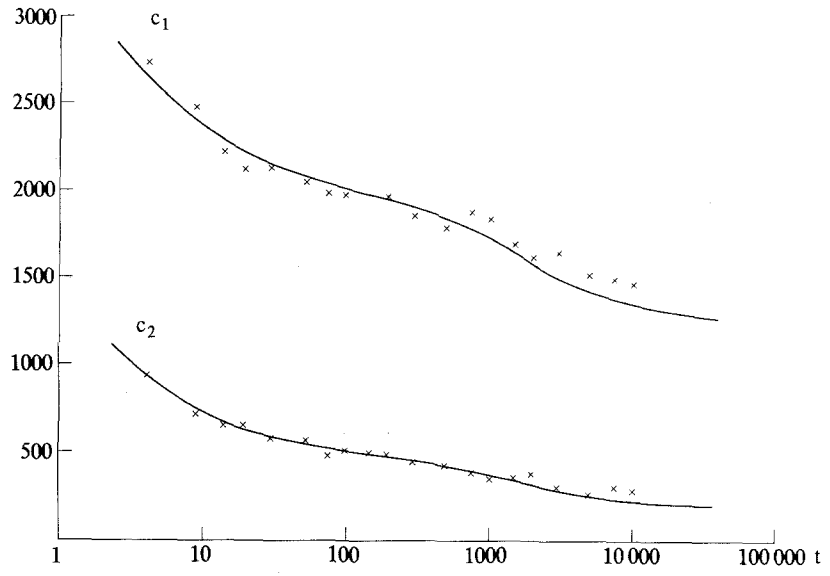

(a)

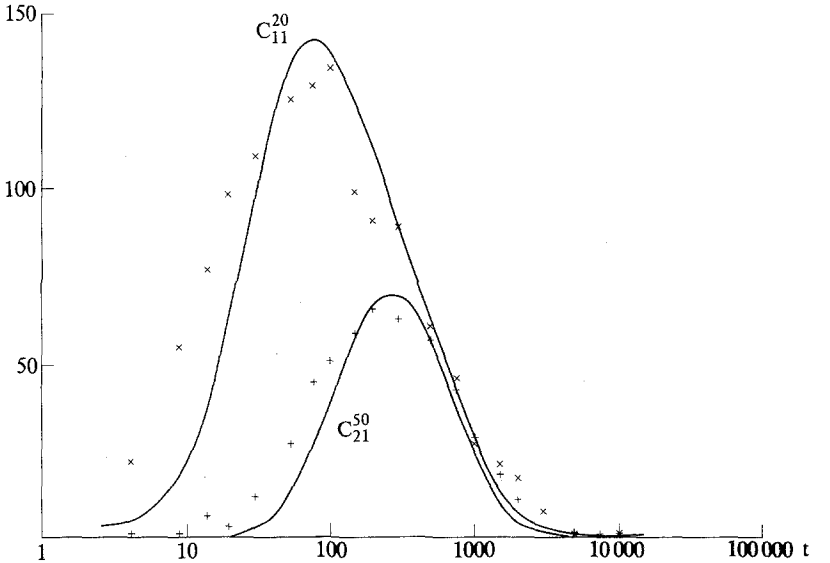

(b)

Fig. 3. Comparison of simulation data (crosses) with predictions of the Becker–Döring equations (curves) at 7.5% density.

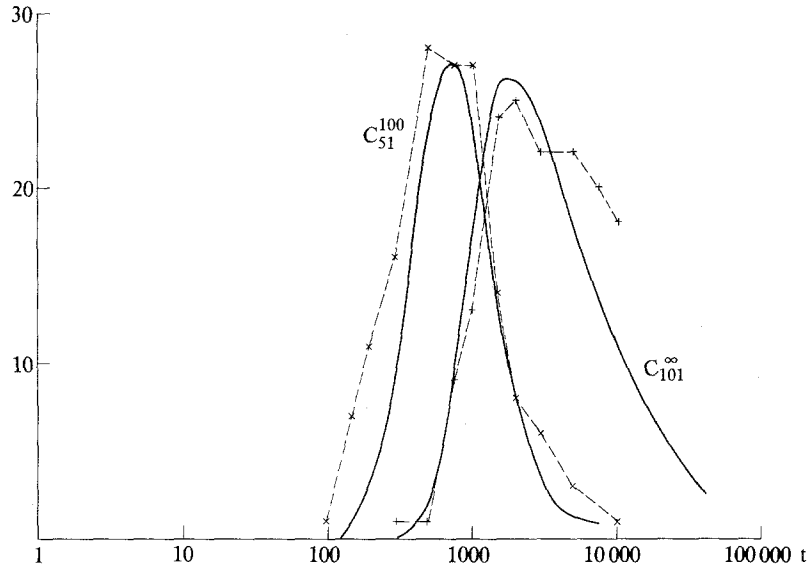

(c)

4.4. Density 10%

Data from the 10% simulation run are shown in Table V, and a comparison with the BD equations is shown in Fig. 4. The data for large clusters could be matched fairly well to the solution of the BD equations by giving to the factor D in Eq. (2.4) the value 2.5, but then the match to the small-cluster data would not be good for times after about 500. No simple scaling of the time axis will imporve the agreement, since the value of c_1 remains near 1600 for a longer time in the simulation than it does in the solution to the BD equations.

5. DISCUSSION

5.1. Finite-System and Fluctuation Effects

The most we can expect from the BD equations is to predict the average behavior of the cluster concentrations c_l obtained from many simulations of very large systems. Our actual simulations reported here on the other hand consist of a single run done on a system containing $N = 125 \times 10^3$ sites and, depending on the density, between 4,375 and

Table V. Simulation at Density 10%

t	c_1	c_2	c_3	c_4	c_5	c_6	c_7	c_8	c_9	c_{10}
0	6666	1278	471	198	83	51	18	13	9	3
3.3	2775	955	497	285	217	126	85	79	44	48
7.3	2346	728	403	249	168	128	97	91	60	47
11.6	2168	608	296	205	171	128	100	72	62	49
16.1	2051	553	287	202	144	133	93	67	49	36
25.5	1939	562	282	175	104	98	61	64	38	38
35.1	1939	535	216	148	130	70	65	55	46	44
45.0	1865	501	236	160	90	60	63	48	43	38
76.0	1907	452	211	107	82	65	45	46	25	30
97.3	1713	457	203	116	71	45	42	26	27	15
152	1758	397	172	89	59	49	32	26	17	24
198	1668	413	173	99	48	40	22	31	31	18
304	1654	377	150	73	49	36	26	17	20	12
505	1610	334	122	70	39	25	22	18	7	14
745	1628	325	126	68	44	20	13	4	9	8
996	1603	308	113	64	35	22	16	11	5	9
1503	1557	319	123	59	38	12	14	7	8	3
2006	1568	299	95	45	14	14	8	6	7	6
3000	1458	281	84	35	10	11	4	2	2	1
4996	1452	271	87	38	19	8	6	3	0	0
7151	1368	245	66	35	19	6	3	1	1	0

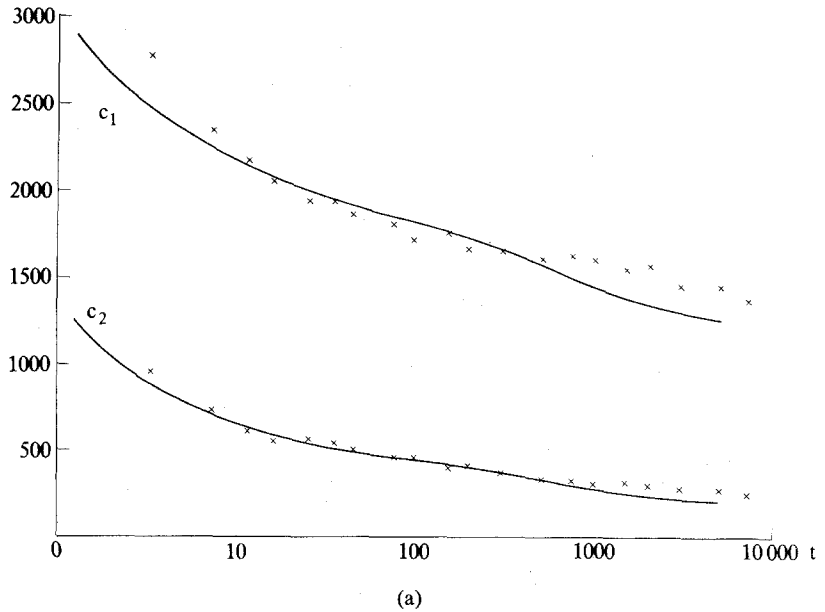

(a)

Fig. 4. Comparison of simulation data (crosses) with predictions of the Becker–Döring equations (curves) at 10% density.

Table V. (Continued)

t	c_1^{10}	c_{11}^{20}	c_{21}^{50}	c_{51}^{100}	c_{101}^{500}	c_{501}^{5000}	N_1^{10}	N_{11}^{20}	N_{21}^{50}	N_{51}^{100}	N_{101}^{500}	N_{501}^{5000}
0	8790	1					12489	11				
3.3	5111	89	2				11260	1194	46			
7.3	4317	153	16				10032	2100	368			
11.6	3859	195	25				9039	2781	680			
16.1	3165	227	37				8332	3187	981			
25.5	3361	227	68				7378	3258	1864			
35.1	3248	218	75	2			7068	3220	2080	132		
45.0	3104	195	98	3			6617	2891	2807	185		
76.0	2870	147	132	8			5780	2171	4081	468		
97.3	2715	149	135	14	1		5220	2171	4140	860	109	
152	2623	132	110	33	2		4838	1932	3371	2136	223	
198	2543	100	109	37	2		4750	1479	3531	2470	270	
304	2414	73	87	42	12		4229	1175	2834	2899	1463	
505	2261	39	62	42	24		3770	553	2146	2932	3099	
745	2255	33	36	38	28		3632	478	1195	2801	4394	
996	2186	20	27	29	37		3456	269	840	2150	5785	
1503	2140	11	12	14	43		3318	144	366	1071	7601	
2006	2062	9	6	11	44		3012	117	161	784	8426	
3000	1888	1	3	4	40		2600	18	112	338	9432	
4996	1884	4	2	4	31	3	2616	49	74	304	7799	1658
7151	1744	0	1	2	27	5	2365	0	45	158	6851	3081

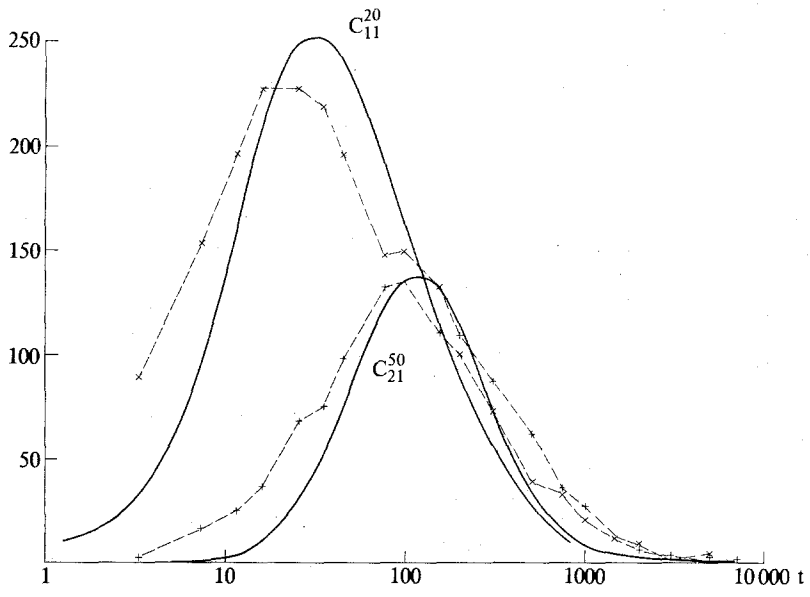

(b)

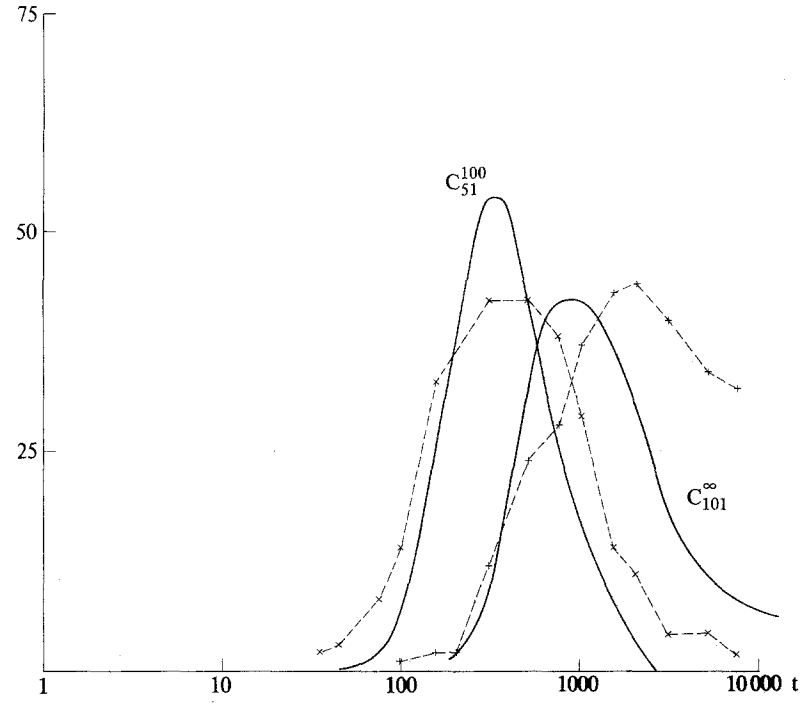

(c)

Fig. 4. Continued.

12,500 particles. We might expect *a priori* that finite-size effects woul become relevant when clusters with concentrations per site of order N^{-1} o less begin to play an important role in the Becker–Döring equations. Thi effect may be significant at the very late stages of our simulations, e.g. between $t = 10{,}000$ and $t = 16{,}000$ in the 3.5% run.

More important for the early and intermediate times are the fluctua tions. The deviations of cluster concentrations from their average value will vary from one simulation run to another, and cannot be predicted i detail. It would be possible to reduce the effect of these deviations b averaging over more than one simulation run, but we did not do thi because it would have required too much computer time. Another way o trying to reduce them is to average the data over limited periods of time For simplicity, we have not done this either for the analysis described i this paper, though the method has been used in other parts of the analysi of these simulation runs. Its disadvantage is that one has to be careful no to average over too long a time interval, otherwise it is no longer possible t see the details of the evolution.

It is desirable to have some estimate of the size of the statistical fluctuations in these simulations, so that when we meet a deviation between the BD equation and the simulations we have some idea whether to attribute it to fluctuations or to a genuine difference between the BD equations and the average they are meant to predict. One way to estimate such fluctuations is to compare the results of different runs at the same density. This is done in Fig. 2, where the circles denote the result of a second run, lasting up to time 300, in addition to the main one. The data from which this contribution to Fig. 2 was drawn are shown in Table IIIa. A comparison of these two runs in Fig. 2 suggests that it is quite possible for two runs to give values of c_1 differing by as much as 50 and values of c_2 differing by 20, and so they may also differ from their expectation values by comparable amounts. These estimates are consistent with the hypothesis that the standard deviation of the observed values of c_l is roughly equal to the square root of their mean; this would hold, for example, if the observed values of c_l had a Poisson distribution.

5.2. Metastability and The Cloud Point

As mentioned in the Introduction, previous experimental tests of the BD theory have been confined to observations of the cloud point—the largest supersaturation at which a metastable state is possible. This is obtained by first estimating the nucleation rate J for large clusters from the BD equations and then finding the value of the density and temperature at which this rate becomes of the order of 1 per observation time per cubic centimeter. The nucleation rate is found to be quite insensitive to the exact value chosen for the observation volume or time since J changes with density and temperature by factors like 10^{20} in the vicinity of the cloud point.

To estimate J from the BD equations one can use an approximate method introduced by Becker and Döring in their 1935 paper.[1] This method assumes that the clusters are in a quasisteady state with J_l in Eq. (2.1) independent of l. We can then deduce from Eq. (2.2) that J, the common value of all the J_l, satisfies

$$c_1 = J\sum_{l=1}^{\infty} \frac{b_2 b_3 \cdots b_l}{a_1 a_2 \cdots a_l} \frac{1}{c_1^l} \cong J\left\{ \frac{1}{a_1 c_1} + \sum_{l=2}^{\infty} \frac{1}{a_l Q_l c_1^l (1-\rho)^{3l-4}} \right\} \quad (5.1)$$

by (2.20). The series, which can be crudely approximated by its largest term, depends very sensitively on the point in the phase diagram to which the system is quenched.

Using the extrapolation formulas (2.4) and (2.6), we find J at density 3.5% to be about 5.4×10^{-10} per site per time unit. The corresponding

critical cluster size l^* [the value of l for which $Q_l c_1^l (1-\rho)^{3l}$ is least] is abou 70. These numbers have the interpretation that, once the metastable state i properly established, the number of clusters of size l^* or larger is increasin at a rate of about 5.4×10^{-10} per site per time unit, which corresponds to a rate of $50^3 J = 6.8 \times 10^{-5}$ per time unit on the $50 \times 50 \times 50$ lattice used i our simulations. We would therefore expect the number of clusters large than 70 to reach the value 1 at about time $(6.8 \times 10^{-5})^{-1} \cong 15{,}000$ According to the detailed BD calculation, on the other hand, the rate o increase of the number of such clusters is smaller by a factor of at least 2 so that even at time 15,000 the expected number of clusters larger than 70 i less than 0.5; and at later times the rate of increase of the number of larg clusters becomes smaller still. It appears that the constant-J *ansatz* whic we used in deriving (5.1), and which is also the keystone of standar nucleation theory, is not a very accurate approximation at the densit considered here (3.5%). Further studies of the mathematical properties o the BD equations should help to elucidate these matters.

5.3. Other Temperatures

One possible application of the work described here is to use the BD equations to predict the behavior of quenched binary alloys at temperature other than $0.59 T_c$. To do this we would need values for the coefficients a and b_l at these other temperatures. A generalization of the formula (2.4) fo a_l to such temperatures is given in Ref. 5, and it would not be difficult t generalize the formula (2.6) for w_l in a similar way since the Q_l for $l \leqslant 1$ are known at all temperatures. It would, however, be impossible to appl the method for temperatures close to the critical temperature, because th densities of minority atoms would become high enough to make percolatio effects important, and the single cluster picture on which our analysis i based would break down.

5.4. Relation to Other Work on These Simulation Runs

Our previous theoretical work on these simulation runs was confine to the run at 7.5% overall density.[5,14] The data analysis in Ref. 1 indicates, as shown in deriving (2.19) above, that for large l

$$a_l \sim 7.5 l^{1/3} \tag{5.2}$$

and the analysis in Ref. 5 indicates that the time variable in the Becker-Döring equation with $D = 1/6$, denoted in Ref. 5 by τ, is related to th time variable t in the simulation by

$$\tau = 3.3(t + 400) \tag{5.3}$$

Equation (2.17) of the present paper, generalized to values of D other than $1/6$, gives

$$a_l \sim 12.36 D l^{1/3}$$

so that (5.2) corresponds to $D = 7.6/12.36 = 0.6$; and the factor 3.3 in (5.3) corresponds (for $t \gg 400$) to $D = 3.3/6 = 0.55$. On the other hand, as noted in Section 4.3 above, the data analysis in the present paper indicates $D \simeq 1$. This discrepancy appears to arise mainly from the fact that in the present paper we did not average out the information from the early times. It seems likely that the effective value of D is larger at earlier times than later, because of the finite time necessary to establish steady-state diffusion near a given large cluster, but we have not attempted to account for this effect here.

We should finally mention that we have no good *a priori* way of comparing our time scale with that of real experiments on quenched binary alloys. Very rough estimates, involving identification of the factor D in Eq. (2.4) with the real diffusion constant in the material, yield a time unit of the order of some seconds for Al–Zn alloys at the temperature $0.59 T_c$. An even greater difficulty arises in any direct comparison of our solution of the BD equations and the time evolution of a supersaturated vapor. The mass flow in the latter system involves not only diffusion but also heat conduction and hydrodynamic flows. These effects could entirely change the l dependence of the coefficients a_l from that given in (2.4). What effect such changes would have on the solutions of the BD equations is not clear to us, although their effect on the formula (5.1) derived using the steady-state *ansatz* would be relatively small since it would only affect the factors a_l in the series, which do not vary nearly as rapidly with l as the factors Q_l and c_1^l.

ACKNOWLEDGMENTS

We are grateful to Dieter Heermann for supplying the simulation data on large clusters used in Table I, to George Gilmer for supplying information about the surface tension of the Ising model, and to Paul Garner for plotting the graphs with the help of a computer.

REFERENCES

1. R. Becker and W. Döring, *Ann. Phys. (Leipzig)* **24**:719–752 (1935).
2. F. F. Abraham, *Homogeneous Nucleation Theory* (Academic Press, New York, 1974).
3. O. Penrose and Joel L. Lebowitz, Towards a Rigorous Theory of Metastablity, in *Fluctuation Phenomena*, E. W. Montroll and J. L. Lebowitz, eds. (North-Holland, Amsterdam, 1979).

4. D. N. Sinha, J. S. Semura, and L. C. Brodie, Homogeneous Nucleation in ^{4}He: A Corresponding-States Analysis, *Phys. Rev. A* **26**:1048–1061 (1982).
5. O. Penrose and A. Buhagiar, Kinetics of Nucleation in a Lattice Gas Model: Microscopic Theory and Simulation Compared, *J. Stat. Phys.* **30**:219–241 (1983).
6. M. Kalos, Joel L. Lebowitz, O. Penrose, and A. Sur, Clusters, Metastability, and Nucleation: Kinetics of First-Order Phase Transitions, *J. Stat. Phys.* **18**:39–52 (1978).
7. J. W. Essam, in *Phase Transitions and Critical Phenomena*, C. Domb and M. S. Green, eds (Academic Press, London, 1972), Vol. 2, p. 197.
8. Joel L. Lebowitz, J. Marro, and M. H. Kalos, Dynamical Scaling of Structure Function in Quenched Binary Alloys, *Acta Metallurgica* **30**:297–310 (1982).
9. D. Stauffer, A. Coniglio, and D. W. Heerman, Monte Carlo Experiment for Nucleation Rate in the Three-Dimensional Ising Model, *Phys. Rev. Lett.* **49**:1299–1302 (1982).
10. H. J. Leamy, G. H. Gilmer, K. A. Jackson, and P. Bennema, Lattice-Gas Interface Structure: A Monte Carlo Simulation, *Phys. Rev. Lett.* **30**:601–603 (1973).
11. I. M. Lifshitz and V. V. Slyozov, *J. Phys. Chem. Solids* **19**:35 (1961); E. M. Lifshitz and L. P. Pitayevskii, *Physical Kinetics* (Pergamon Press, New York, 1981), pp. 427–438.
12. P. Fratzl, J. L. Lebowitz, J. Marro, and M. H. Kalos, The Interpretation of Structure Functions in Quenched Binary Alloys, *Acta Metallurgica* **31**:1849–1860.
13. D. W. Heerman and W. Klein, Nucleation and Growth of Nonclassical Droplets, *Phys. Rev. Lett.* **50**:1062–1065 (1983).
14. O. Penrose, Joel L. Lebowitz, J. Marro, M. H. Kalos, and A. Sur, Growth of Clusters in a First-Order Phase Transition, *J. Stat. Phys.* **19**:243–267 (1978); erratum, *ibid.* **24**:70 (1981).
15. J. Marro and R. Toral, Equilibrium Cluster Distribution of the 3-Dimensional Ising Model in the One-Phase Region, *Physica A* **122A**:563–586.
16. M. Aizenman, F. Delyon, and B. Souillard, Lower Bounds on the Cluster Size Distribution, *J. Stat. Phys.* **23**:267 (1980).